

# Excitation and dissociation of SF<sub>6</sub> molecules in a two-frequency infrared laser field

S. S. Alimpiev, B. O. Zikrin, B. G. Sartakov, and É. M. Khokhlov

*P. N. Lebedev Physics Institute, USSR Academy of Sciences*

(Submitted 26 March 1982)

Zh. Eksp. Teor. Fiz. **83**, 1634–1649 (November 1982)

The spectral and energy characteristics of the excitation and dissociation of SF<sub>6</sub> molecules in a two-frequency infrared laser field are investigated. The quantum efficiency of two-frequency dissociation is found to depend on the frequency of the second field and on the excitation level in the first. The linear-absorption spectra of SF<sub>6</sub> molecules excited by a laser field are obtained. The parameters of these spectra differ significantly from the thermal ones.

PACS numbers: 33.20.Ea, 33.80.Gj

## I. INTRODUCTION

The procedure of double IR resonance has found extensive use in the investigation of resonant excitation of molecules in a laser field. First used to investigate relaxation processes upon excitation of lower vibrational levels of molecules,<sup>1</sup> double IR resonance found extensive application in research into multistep excitation of molecules in a strong IR laser field.

The gist of the procedure consists in using two IR fields that are usually of different intensity and frequency. The first is the exciting field and produces an ensemble of excited molecules and the second is the sounding field and investigates the behavior of this ensemble.

The main results of the procedure is the linear absorption spectrum of excited molecules. Comparison of this spectrum with the spectrum of the thermally heated gas indicates whether the laser and nonlaser heating methods are equivalent. Moreover, an analysis of the shape of the spectrum of the excited molecules yields information on the character of the distribution of the populations among the vibrational levels and on the distribution of the energy absorbed by the molecule among the vibrational degrees of freedom.

The capabilities of the double IR resonance technique are considerably extended by using an intense laser radiation as the second field.<sup>2,3</sup> In this case the procedure makes it possible not only to follow the behavior of the ensemble of excited molecules, but also to search for the best ways of further excitation of the molecules in the region of the quasi-

continuum of the high vibrational states, and also to investigate the efficiency of their dissociation under different excitation conditions.

Thus, the use of the double IR resonance technique makes it possible answer a large number of questions that are of fundamental importance from the point of view of understanding the mechanism and optimizing the process of multistep excitation and dissociation of polyatomic molecules in an IR laser field. The present paper is devoted to an investigation of the excitation of high vibrational levels and to the dissociation of SF<sub>6</sub> molecules using the double IR resonance technique.

## II. EXPERIMENTAL SETUP

A diagram of the experimental setup is shown in Fig. 1. We used two CO<sub>2</sub> atmospheric-pressure transverse-discharge lasers. The instants of lasing were synchronized, and the delay between the pulses was adjustable in a wide range. The standard gas mixture CO<sub>2</sub>:N<sub>2</sub>:He = 1:0.3:3 used in lasers was poorer in nitrogen, thus considerably shortening the tail part of the pulse. The laser frequencies were tunable by diffraction gratings relative to the CO<sub>2</sub> lines. The frequency range of the second laser L<sub>2</sub> was greatly broadened by using isotopically substituted gas <sup>13</sup>CO<sub>2</sub> and also by converting the emission of a CO<sub>2</sub> laser L<sub>2</sub> by using it to pump an NH<sub>3</sub> laser.<sup>4</sup> The use of <sup>13</sup>CO<sub>2</sub> gas makes it possible to obtain a number of frequencies in the 880–920 cm<sup>-1</sup> band, frequencies not attainable with an ordinary CO<sub>2</sub> laser. The NH<sub>3</sub> laser generat-

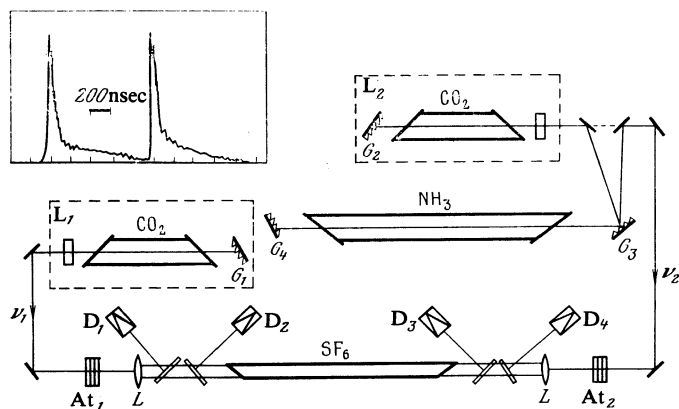


FIG. 1. Diagram of experimental setup.

ed a number of frequencies in the 790–880  $\text{cm}^{-1}$  range, with laser energy 50–200 mJ at a pulse duration practically coinciding with the pump-pulse duration. The optical system of the  $\text{NH}_3$  laser consists of two gratings  $G_3$  (100 lines/mm) and  $G_4$  (150 lines/mm) and a semitransparent KCl mirror. The diffraction grating  $G_4$  guides pump radiation of 9.3  $\mu\text{m}$  wavelength (the P30 line) into a cell with  $\text{NH}_3$  in the first diffraction order, and extracts, without diffraction losses, the laser radiation in the first order. An advantage of this system is that the direction of the  $\text{NH}_3$  laser output remains unchanged when its frequency is tuned by rotating the grating  $G_3$ .

The laser beams are directed into a cell with the aid of long-focus lenses  $L$  ( $F = 50\text{--}100$  cm). The energy of the laser pulses is monitored and measured with the aid of cavity-type pyroelectric calorimeters  $D_1\text{--}D_4$ , placed in channels branched by means of beam splitters, and a similar calorimeter mounted in the direct beam. Particular attention was paid to the absolute calibration of the calorimeter; the total calorimetry error did not exceed 5%. The radiation was attenuated within a wide range with the aid of  $\text{CaF}_2$  plates.

In most experiments we used a waveguide-type cell constituting a tube of stainless steel 50 cm long and 5 mm inside diameter, with a polished internal surface. The cell was sealed with Brewster windows of thin  $\text{BaF}_2$  plates. The transmission coefficient of the cell without the gas and the radiation filling factor were close to unity.

The use of a waveguide-type cell offers a number of advantages. First, in this case the region of interaction of the laser radiation with the gas is fully defined; second, the fact that a limited volume is used for the interaction excludes processes wherein the excited molecules move apart, and replaces these processes by the slower diffusion towards the wall. This extends the time range and results in more correct relaxation measurements. In addition, the procedure makes it possible to measure the probability of molecule dissociation in a laser field by irradiating the cell only once.

Most experiments were performed with the cell filled with a gas mixture  $\text{SF}_6\text{:H}_2 = 1\text{:}1$  at a total pressure 1 Torr. The presence of hydrogen as the atomic-fluorine acceptor stabilizes the dissociation of the  $\text{SF}_6$  molecules, and makes this process insensitive to the state of the cell walls. Further increase of the partial pressure of the hydrogen leads to gradual lowering of the dissociation probability on account of  $V\text{--}T$  relaxation within an excitation time determined principally by the delay between the exciting pulses.

The cell was evacuated by an NORD-100 magnetoionization pump.

The optical system employed made it possible to measure the absorbed energy separately from the first and second fields ( $\bar{\nu}_1$  and  $\bar{\nu}_2$ ) and the corresponding probability  $W$  of molecule dissociation. The absorbed-energy measurement unit in all the experiments, at all excitation frequencies, was the number of photons of frequency 944.2  $\text{cm}^{-1}$  absorbed per  $\text{SF}_6$  molecule.

The procedure for measuring  $W$  consisted of sounding the concentration of the residual  $\text{SF}_6$  gas a few seconds after the irradiation. The sounding radiation was produced by the 944.2  $\text{cm}^{-1}$  exciting laser  $L_1$  whose intensity was attenuated

to  $\Phi_0 = 4$   $\text{mJ}/\text{cm}^2$ . The dissociation probability was determined from the relation

$$W = 1 - N_f/N_i,$$

where  $N_i$  and  $N_f$  are the initial and final densities of the  $\text{SF}_6$ , determined by measuring the transmission of the sounding radiation

$$\Phi_{i,f} = \Phi_0 \exp(-\sigma l N_{i,f}).$$

By sounding the mixtures having different  $\text{SF}_6\text{:H}_2$  ratios and with other buffer gases it was established that the absorption cross section  $\sigma$  does not depend on the  $\text{SF}_6$  concentration and, within the accuracy limits, also on the type of buffer gas, but depends strongly on the total pressure of the mixture,  $\sigma(P) \sim P^{0.5}$ . The dependence of the absorption cross section on the pressure is the consequence of the nonlinearity of the absorption of the sounding radiation. Thus, at the employed energy densities  $\Phi_0 \approx 4$   $\text{mJ}/\text{cm}^2$  the absorption cross section was  $\sigma = 1.8 \times 10^{-18}$   $\text{cm}^2$  at a linear absorption cross section  $\sigma_{\text{lin}} \approx 1.3 \times 10^{17}$   $\text{cm}^2$ . Linear absorption was achieved at 944.2  $\text{cm}^{-1}$  by considerably decreasing  $\Phi_0$ , but measurement of the  $\text{SF}_6$  concentration at the  $\text{SF}_6$  pressures used in the experiment, namely  $P \approx 0.5$  Torr, is made difficult by the high density of the sample [the attenuation is  $\exp(\sigma_{\text{lin}} l N) \approx 10^7$ ].

The dependence of the cross section for the absorption of the sounding radiation on the pressure was taken into account when determining the dissociation probability, since it has been established that the pressure of the mixture decreased appreciably in the cell after the irradiation, obviously as the result of deposition of the dissociation products on the cell walls. To correct the values of  $W$ , we measured the residual-gas pressure after the irradiation, and the corrected value  $W'$  was determined from the relation

$$W' = 1 - (\sigma_i/\sigma_f) (N_f/N_i),$$

where  $\sigma_i$  and  $\sigma_f$  are the cross sections for the absorption of the sounding radiation before and after the irradiation.

The sounding procedure was used also to investigate the spectra of the linear absorption of  $\text{SF}_6$  molecules excited beforehand in the field of the first laser. The sounding field employed was the appreciably attenuated pulse of the second laser, delayed relative to the excitation pulse by 1  $\mu\text{sec}$ . The energy density of the sounding pulse was chosen to satisfy the condition that the absorption be linear, and did not exceed 1  $\text{mJ}/\text{cm}^2$ . The absorption linearity was verified by transferring part of the attenuating  $\text{CaF}_2$  plates of the attenuator  $\text{At}_2$  directly to the input of the calorimeter  $D_2$ ; this increased the sounding-energy density. The fact that the signal of the calorimeter  $D_2$  remained constant in this operation was evidence of linearity of the absorption. A substantial advantage of the use of a cell of the wavelength type in these experiments is the complete elimination of the possibility of sounding the unexcited or weakly excited molecules on the wings or outside the volume illuminated by the first field.

### III. EXPERIMENTAL RESULTS

#### 1. Single-frequency excitation

In the first series of experiments we measured the energy absorbed by the  $\text{SF}_6$  gas and the probability, correspond-

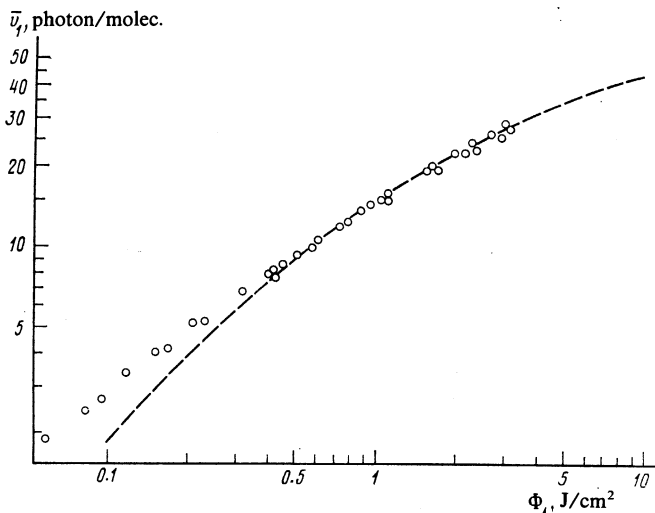


FIG. 2. Dependence of the average absorbed energy of SF<sub>6</sub> on the laser-field energy density. Points:  $\nu = 944.2 \text{ cm}^{-1}$ ; SF<sub>6</sub>:H<sub>2</sub> = 1:1,  $P_x = 1 \text{ Torr}$ . Dashed curve—data of Ref. 5.

ing to this absorption, of the dissociation in the single-frequency regime at various excitation energy densities at the frequency  $\nu_1 = 944.2 \text{ cm}^{-1}$ .

Figure 2 shows the dependence of the average absorbed energy  $\bar{\nu}_1$  per SF<sub>6</sub> molecule on the average energy density  $\Phi_1$  at the entrance into and exit from the cell. In the averaging it was taken into account that the transmission coefficient  $T$  of the cell with the gas depends on the excitation-energy density and falls off monotonically from  $T = 0.9$  at  $\Phi_{in} = 3 \text{ J/cm}^2$  to  $T = 0.6$  at  $\Phi_{in} = 0.07 \text{ J/cm}^2$ . The character of the  $\bar{\nu}_1(\Phi_1)$  dependence (Fig. 2) changes from  $\bar{\nu}_1 \sim \Phi^{0.75}$  at  $\Phi_1 = 0.1 \text{ J/cm}^2$  to  $\bar{\nu}_1 \sim \Phi^{0.5}$  near  $\Phi_1 = 3 \text{ J/cm}^2$ . The dashed line in Fig. 2 shows the results of similar measurements carried out by us earlier<sup>5</sup> in a cell of ordinary type in a somewhat larger range of energy densities. The curves are in good agreement. The differences at low energy densities are apparently due to the dependence of the absorbed energy on the pressure, due to the influence of the relaxation on the effectiveness of passage through the low vibrational levels, contribution of the relaxation being noticeable only at low energy densities  $\Phi_1 < 0.4 \text{ J/cm}^2$  and decreasing with increasing excitation energy.

Figure 3 shows the dependence of the SF<sub>6</sub> dissociation probability on the average energy density  $\Phi_1$  in the single-frequency regime (curve 1) and, for comparison, in the two-frequency excitation regime (curve 2), on the summary energy density of the two fields  $\Phi_1 + \Phi_2$ . The dashed curve in the figure shows the data obtained by us in Ref. 5 in an ordinary cell using the traditional procedure of measuring  $W$  by IR spectrometry of the residual gas SF<sub>6</sub> after multiple irradiation of the cell.

The appreciable difference between curves 1 and 3 (see Fig. 3) can be the consequence of several factors. First, it is possible that owing to the fast resonant  $V-V$  exchange<sup>6</sup> of the excited SF<sub>6</sub> molecules with the dissociation products SF<sub>4</sub>, S<sub>2</sub>F<sub>10</sub>, SOF<sub>2</sub>,... that accumulate in the course of the irradiation, the excitation level of the SF<sub>6</sub> is lowered, and consequently the dissociation probability measured by averaging

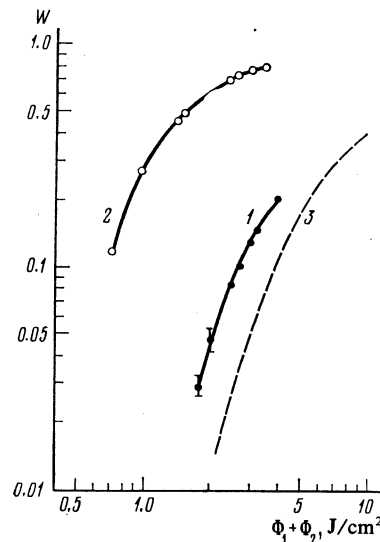


FIG. 3. Dependence of the dissociation probability on the total excitation energy density: 1—in the single-frequency regime,  $\Phi_2 = 0$ ; 2—in the two-frequency regime,  $\nu_1 = 944.2 \text{ cm}^{-1}$ ,  $\nu_2 = 888 \text{ cm}^{-1}$ ,  $\Phi_1 = 0.5 \text{ J/cm}^2$ ; 3—single-frequency regime, data of Ref. 5.

over a large number of shots is decreased. This effect can be one of the causes of the decreases, observed in Ref. 7, of the value of  $W$  of SF<sub>6</sub> gas in each succeeding excitation act.

The second cause of the observed differences may be the considerably slower cooling of the gas after excitation in a cell of the waveguide type, and consequently of the larger contribution made to  $W$  by the collisional or thermal phase of the dissociation. Indeed, a sufficiently rapid  $V-T$  relaxation in the presence of hydrogen, leading to heating of the translational degrees of freedom, can lower the gas temperature only insignificantly owing to the relatively low heat capacity of the degrees of freedom that are added. The main gas-cooling process, on the other hand, in a cell of the waveguide type, is slow diffusion of the hot molecules towards the walls. In a cell partially filled with radiation, heating of the translational degrees of freedom leads to a considerable increase of the pressure in the region of the focal constriction. As a result, the gas broadens rapidly and is cooled, for example, on account of  $V-V$  relaxation with the unexcited molecules.

That a contribution is made to  $W$  by the collisional state of dissociation is indicated by the experimentally observed decrease of  $W$  with increasing partial pressure of the hydrogen in the mixture. Thus, in the regime of moderate single-particle excitation, the change of the ratio of the gases SF<sub>6</sub>:H<sub>2</sub> from 1:1 to 1:3, by increasing the heat capacity of the reservoir, leads to a twofold decrease of  $W$  from 8 to 4%. On the other hand, a change of the total pressure of the mixture in both cases in the range 0.5–2 Torr does not change the value of  $W$ .

The dependence of  $W$  on the SF<sub>6</sub> concentration can be the second cause of the decrease of  $W$  in each succeeding pulse in the repeated-irradiation regime, for as the SF<sub>6</sub> gas is spent, in the presence of an acceptor, the ratio of the gases obviously changes. We note also that the dependence of  $W$  on the SF<sub>6</sub>:H<sub>2</sub> ratio is observed only at moderate levels of

radiative excitation, and vanishes under conditions of two-frequency dissociation of the molecules.

A comparison of curves 1 and 2 in Fig. 3 shows a considerable increase of the probability of the  $SF_6$  dissociation under conditions of two particle excitation when the frequency of the second field is lowered.<sup>3</sup> Thus, at a total energy density  $\Phi_1 + \Phi_2 = 1 \text{ J/cm}^2$  of the two-frequency (case II) excitation, which is easily realized in unfocused  $CO_2$ -laser beams, the dissociation probability is  $W_{II} = 0.26$ , and the gain relative to the single-frequency (case I) irradiation regime  $W_{II}/W_I$  reaches several orders of magnitude: in the  $W_{II}$  saturation region at  $\Phi_1 + \Phi_2 = 3 \text{ J/cm}^2$  the gain is  $W_{II}/W_I = 6$ . These results point to the need for a detailed investigation of the spectral and energy characteristics of the dissociation of the molecules in the two-frequency excitation regime.

## 2. Two-frequency dissociation of $SF_6$

Figure 4 shows the dependences of the dissociation probability and of the energy absorbed from the second field as the frequency of the latter is changed in the range 790–950  $\text{cm}^{-1}$ . The spectra were obtained at a fixed second-field energy density  $\Phi_2 = 0.15 \text{ J/cm}^2$  and at an excitation level in the first field  $\Phi_1 = 2.7 \text{ J/cm}^2$ , with  $\bar{\nu}_1 = 25$  photon/molec. The maximum of the  $W(\nu_2)$  curve is reached near  $\nu_2 = 850 \text{ cm}^{-1}$ , i.e., it is shifted relative to the frequency of the main transition  $\nu_{01} = 948 \text{ cm}^{-1}$  by  $\sim 100 \text{ cm}^{-1}$ .

The positions of the maxima of the curves depend on the excitation level in the first field. Thus, in the analogous spectra obtained at  $\Phi_1 = 0.5 \text{ J/cm}^2$  and  $\bar{\nu}_1 = 9$  photon/molec. the  $W(\nu_2)$  dependence has a maximum near  $\nu_2 = 885 \text{ cm}^{-1}$ , while the absorbed-energy curve  $\bar{\nu}_2(\nu_2)$  has a maximum at  $905 \text{ cm}^{-1}$ . Attention is called to the absence of correlation between the spectral dependence of  $W$  and  $\bar{\nu}_2$ , so that the ratio  $W/\bar{\nu}_2$ , which characterizes the efficiency of the action of the second field, grows monotonically with increasing long-wave shift of its frequency.

To explain the causes of this effect, we investigated the  $W(\Phi_1, \Phi_2)$  and  $\bar{\nu}_1(\Phi_1, \Phi_2)$  dependences in a wide range of energy densities  $\Phi_1$  and  $\Phi_2$  of the exciting fields and at various frequencies  $\nu_2$  of the second field. The results are shown in Figs. 5a and 5b.

Figure 5a shows plots of  $W(\Phi_2)$  and  $\bar{\nu}_2(\Phi_2)$  for two excitation levels in the first field,  $\bar{\nu}_1 = 9$  photon/molec. and  $\bar{\nu}_1 = 21$  photon/molec., and at excitation frequencies

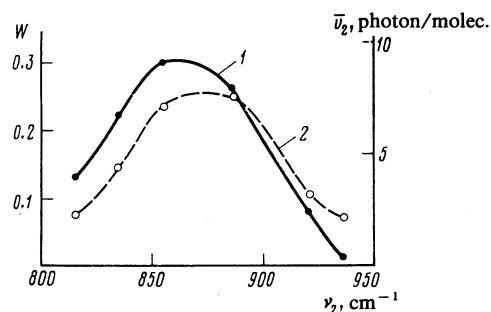
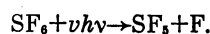


FIG. 4. Dependences of the dissociation probability (1) and of the energy absorbed (2) from the second field on its frequency.  $\Phi_2 = 0.15 \text{ J/cm}^2$ ;  $\Phi_1 = 2.7 \text{ J/cm}^2$ ,  $\bar{\nu}_1 = 25$  photon/molec.

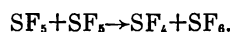
$\nu_1 = 944.2$  and  $\nu_2 = 896.9 \text{ cm}^{-1}$ . Figure 5b shows the  $W(\nu_1)$  dependence at a fixed value of the energy density of the second field  $\Phi_2 = 2 \text{ J/cm}^2$ . An analysis of the curves of Fig. 5 shows that the functions  $W(\Phi_1)$  and  $W(\Phi_2)$  saturate both when  $\Phi_1$  (Fig. 5b) and  $\Phi_2$  (Fig. 5a) increase, but the value of  $W$  in the saturation region,  $W_s = 0.82$ , i.e., is noticeably less than unity. Lowering the excitation level in the first field from  $\bar{\nu}_1 = 21$  to  $\nu_1 = 9$  photon/molec. (Fig. 5b) does not decrease  $W_s$ .

The fact that the observed value  $W_s < 1$  could be explained by the presence of a "cold" ensemble of molecules<sup>8,9</sup> (molecule fraction  $q = 0.18$ ) that remain in the system of lower vibrational levels and do not absorb the radiation of the second laser whose frequency is shifted towards the red side. However, the saturation of the  $W(\Phi_2)$  dependence (Fig. 5a) and the independence of  $W_s$  of the excitation level in the first field patently contradict this hypothesis, since it is necessary in this case to assume that  $q$  does not depend on the excitation level in the first field, i.e., 18% of the molecules absorb neither the first resonant nor the second detuned field.

The most probable, in our opinion, explanation of the difference between  $W_s$  and unity is the recombination of the products of the radiative dissociation

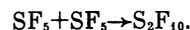


Thus, the formation of the  $SF_6$  molecules is due to the recombination process considered in Ref. 10:



Since the sounding of the residual  $SF_6$  gas is carried out several seconds after the irradiation, the  $SF_6$  molecules produced via this channel lower the measured value of the dissociation probability.

An obvious method of suppressing the recombination of the dissociation products is to choose acceptors that bind the  $SF_6$  radical. However, addition of the gases  $H_2$ ,  $H_2O$ ,  $O_2$ ,  $N_2O$ , and  $N_2F_4$  do not lead to an increase of  $W_s$ , thus apparently indicating that the employed gases, being good acceptors for atomic fluorine, do not bind the radical  $SF_5$  and the principal channel of  $SF_5$  binding is the reaction



It is obvious at the same time that the number of the  $SF_6$  molecules newly produced as a result of recombination is proportional to the concentration of the  $SF_5$  and consequently to the probability  $W$  of the radiative recombination. Therefore the recombination makes an additive contribution and the real value of  $W$  can be obtained by simple renormalization of the measured values.

Plots of  $W(\Phi_1, \Phi_2)$  and  $\bar{\nu}(\Phi_1, \Phi_2)$  similar to the curves of Fig. 5 were obtained at a number of second-field frequencies in the range 950–880  $\text{cm}^{-1}$ . The change of the frequency of the second field leads primarily to a change in the absorption cross section in the quasicontinuum and, consequently, to a substantial shift of the  $W(\Phi)$  and  $\bar{\nu}(\Phi)$  curves along the energy-density scale. The character of the change of the absorption cross section is clear from an analysis of the spectral dependences (Fig. 4), and it is therefore of interest to analyze

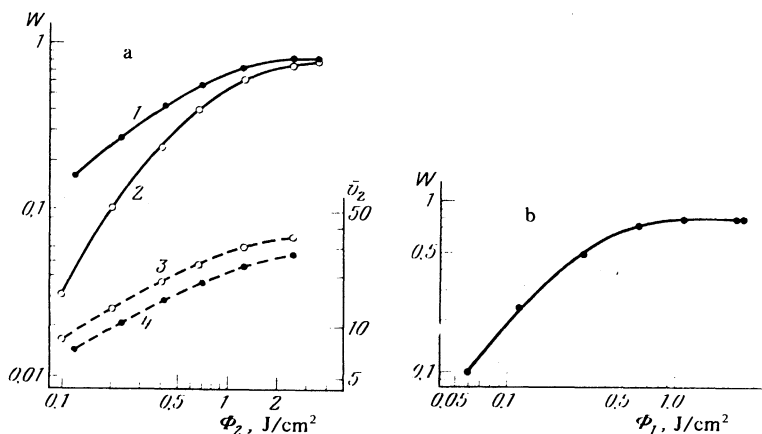


FIG. 5. (a) Dependences of the dissociation probability (1, 2) and of the energy absorbed from the second field (3, 4) on the energy density of the field for two excitation levels in the first field: 1, 4)  $\bar{\nu}_1 = 21$  photon/molec.; 2, 3)  $\bar{\nu}_1 = 9$  photon/molec.,  $\nu_2 = 897 \text{ cm}^{-1}$ . b) Dependence of the dissociation probability on the energy density of the first field  $\Phi_1$  at  $\Phi_2 = 2.0 \text{ J/cm}^2$  and  $\nu_2 = 888 \text{ cm}^{-1}$ .

the  $W(\bar{\nu})$  dependences, which are not sensitive to the value of the absorption cross section and describe the quantum efficiency of the dissociation.

The functions  $W(\bar{\nu}_1 + \bar{\nu}_2)$  are shown in Fig. 6 for three different second-field frequencies  $\nu_2 = 886.1$ ,  $896.9$ , and  $923.1 \text{ cm}^{-1}$ , and for two excitation levels in the first field,  $\bar{\nu}_1 = 9$  and  $21$  photon/molec. Analysis of the curves shows that the dissociation probability is determined not only by the averaged level of the absorbed energy  $\bar{\nu} = \bar{\nu}_1 + \bar{\nu}_2$ , but depends also on the excitation method, i.e., on the frequency of the second field and on the ratio of the absorbed energies from the first and second fields.

Thus, at the same summary excitation level  $\bar{\nu}_1 + \bar{\nu}_2$  the

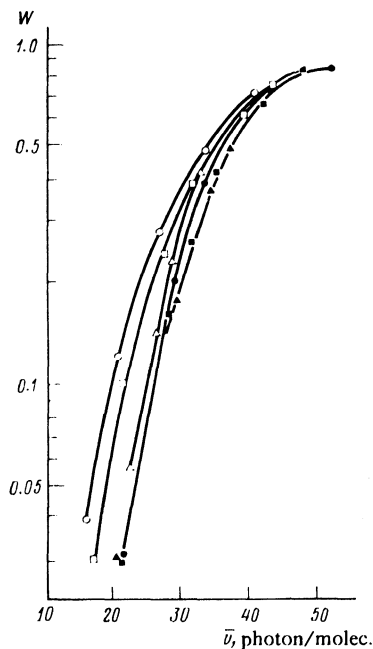


FIG. 6. Dependences of the dissociation probability of  $\text{SF}_6$  on the total energy absorbed for two excitation levels in the first field (light symbols— $\bar{\nu}_1 = 9$  photon/molec., dark symbols— $\bar{\nu}_1 = 21$  photon/molec.) and three frequencies of the second field (points:  $\nu_2 = 886.1 \text{ cm}^{-1}$ , squares— $\nu_2 = 896.9 \text{ cm}^{-1}$ ; triangles— $\nu_2 = 923.1 \text{ cm}^{-1}$ ).

dissociation probability is higher the lower the level of the preliminary excitation  $\bar{\nu}_1$ . With increasing long-wave frequency shift of the second field, the  $W(\bar{\nu}_1 + \bar{\nu}_2)$  curves are deflected to the left, i.e., to obtain a fixed value it is necessary to have a ever small absorbed energy. This fact is clearly pronounced at  $\bar{\nu}_1 = n$  photon/molec. and becomes less noticeable when  $\bar{\nu}_1$  increases to  $21$  photon/molec.

Figure 7 shows plots of the dissociation quantum efficiency  $\beta$ , defined as  $\beta = WD/\bar{\nu}$ , against the average level of the absorbed energy  $\bar{\nu} = \bar{\nu}_1 + \bar{\nu}_2$ . Here  $D$  is the dissociation energy of  $\text{SF}_6$  molecule,  $D = 93 \text{ kcal/mol}$  (Ref. 11), or  $D \approx 34$  photon/molec. ( $\nu = 944.2 \text{ cm}^{-1}$ ). In the plot account is taken of the earlier assumption that  $W_s = 1$ . An analysis of the  $\beta(\bar{\nu}_1 + \bar{\nu}_2)$  curves shows that at relatively low absorption levels the quantum efficiency of the dissociation depends significantly on the excitation method.

Thus, at  $\bar{\nu}_1 + \bar{\nu}_2 = 21$  photons/molec. the quantum effi-

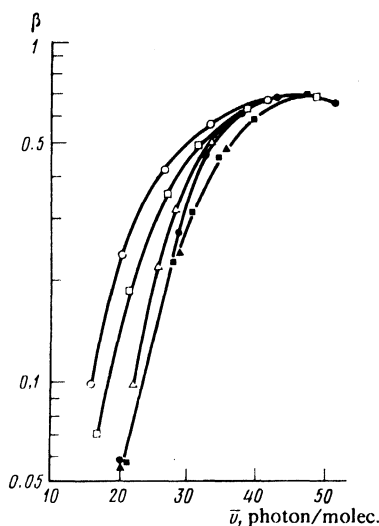


FIG. 7. Dependence of the quantum efficiency of  $\text{SF}_6$  dissociation on the total absorbed energy for two excitation levels in the first field (light symbols— $\bar{\nu}_1 = 9$  photon/molec., dark symbols— $\bar{\nu}_1 = 21$  photon/molec.) and three second-field frequencies (points— $\nu_2 = 886.1 \text{ cm}^{-1}$ , squares— $\nu_2 = 896.9 \text{ cm}^{-1}$ ; triangles— $\nu_2 = 923.1 \text{ cm}^{-1}$ ).

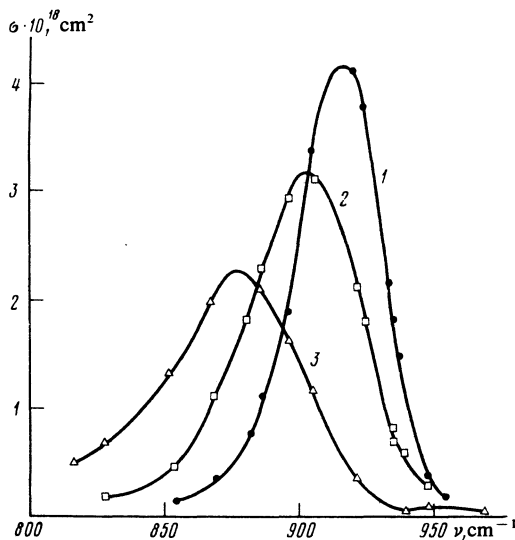


FIG. 8. Spectra of linear absorption of SF<sub>6</sub> gas excited in a laser field to the levels: 1)  $\bar{\nu} = 8.4$  photon/molec.; 2)  $\bar{\nu} = 13.4$  photon/molec.; 3)  $\bar{\nu} = 25$  photon/molec. Delay time  $\tau_3 = 1 \mu\text{sec}$ , SF<sub>6</sub>:H<sub>2</sub> = 1:1, pressure  $P_x = 1$  Torr.

ciency differs by four times, depending on whether this energy is accumulated in fields whose frequency were close to the 0–1 resonance, or if the second-field frequency is shifted by  $\sim 60 \text{ cm}^{-1}$  in the red direction. It can be concluded from this, however, that the gain in  $W$ , obtained through the use of two-frequency dissociation (see Fig. 3) is due not only to the increased absorption cross section in the quasicontinuum following the red shift of the second-field frequency, but also to the substantially higher quantum efficiency of the dissociation in this case.

The main cause of the dependence of the quantum efficiency on the excitation method is, in our opinion, the formation of a specific distribution of the level populations under the conditions of the two-frequency action. The character of this distribution will be considered in detail in Sec. IV.

When the excitation level  $\bar{\nu}$  is raised to values above the dissociation energy  $D$ , the quantum efficiencies become equalized, and a value  $\beta = 0.70$  is reached. From this we can determine that energy excess  $\Delta\bar{\nu}$  which must be imparted to

the SF<sub>6</sub> molecules for dissociation with  $W = 1$  and  $\Delta\bar{\nu} = 14$  photons/molec. This is much higher than the  $\Delta\nu = 9$  photons/molec. obtained in Ref. 12 from an analysis of the energy of the translational motion of the radicals and under the assumption that the energy is uniformly distributed over all the degrees of freedom of the dissociating complex. However, a contribution can be made to the  $\Delta\bar{\nu}$  as measured by us also by the absorption of energy by the SF<sub>5</sub> radicals produced in the course of the dissociation of the SF<sub>6</sub>.

### 3. Sounding of excited states of molecules

Figure 8 shows the results of sounding of SF<sub>6</sub> molecules excited in a single-frequency field with  $\nu = 944.2 \text{ cm}^{-1}$  to various average levels  $\bar{\nu} = 8, 14$ , and 25 photons/molec., by the procedure described in Sec. II. Just as in all the preceding experiments, we investigated the gas mixture SF<sub>6</sub>:H<sub>2</sub> = 1:1 at a total pressure 1 Torr. The sounding pulse was delayed by  $1 \mu\text{sec}$ . The sounding energy density was chosen at each frequency such that the absorption was linear.

With increasing excitation level, the spectra (see Fig. 8) broaden and shift to the long-wave side; the cross section integrated over the spectrum  $A = \int \sigma(\nu) d\nu$  is preserved ( $A = 1.7 \times 10^{-16} \text{ cm}$ ), although it is somewhat lower than the integrated cross section for the fundamental 0–1 transition.<sup>13</sup> Attention is called to a low cross section for the absorption of the excited molecules near the fundamental-transition frequency. This confirms the earlier conclusion that there is no “cold” ensemble of molecules under the experimental conditions ( $T = 300 \text{ K}$ ,  $P_x = 1$  Torr,  $\tau_3 = 1 \mu\text{sec}$ ,  $\Phi_1 > 0.4 \text{ J/cm}^{-2}$ ,  $\nu = 944.2 \text{ cm}^{-1}$ ).

Figures 9a and 9b show plots of the shift  $\nu_{\text{max}} - \nu_0$  of the maximum of the spectrum and of its width  $\Delta\nu_{1/2}$  at half maximum from the average level of the absorbed energy  $\bar{\nu}$ , and also the values of these quantities normalized to the number of absorbed photons. In addition, the figures show plots of  $\nu_{\text{max}} - \nu_0$  and  $\Delta\nu_{1/2}$  from Refs. 14 and 15 on non-laser heating of SF<sub>6</sub> (curves 1' and 2'). Comparison of the plots points to substantial differences between the parameters of the spectra obtained by us and the thermal spectra. These differences are maximal at low excitation levels,  $\bar{\nu} \approx 10$  photons/molec., but when  $\bar{\nu}$  increases to 25 photons/molec., the parameters of the spectrum approach the thermal values.

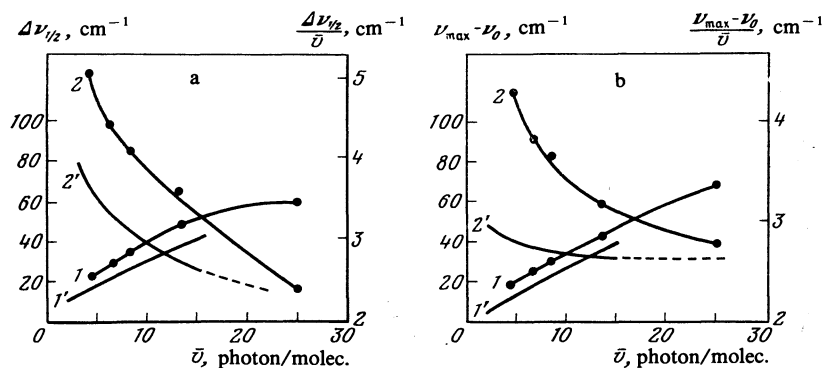


FIG. 9. a) Shift of the maximum of the absorption spectra (curve 1) and shift normalized to  $\bar{\nu}$  (curve 2) as functions of the excitation level of the SF<sub>6</sub> molecules in laser field. b) Widths (curve 1) of absorption spectra and widths (curve 2) normalized to  $\bar{\nu}$ , as functions of the excitation level of the SF<sub>6</sub> molecules in the laser field. 1', 2') Analogous plots from Refs. 14 and 15 obtained by spectroscopy of SF<sub>6</sub> heated in shock tubes.

This manifests itself in particular when the normalized plots 2 and 2' are compared.

#### IV. DISCUSSION OF RESULTS

In the analysis of the experimental results we start from the simplest model, assuming that the cross section for linear absorption, on going from a state with energy  $\nu$  into a state with energy  $\nu + 1$  is determined by the expression

$$\begin{aligned}\sigma(\nu \rightarrow \nu+1) &= A_{01} g(\nu, \nu) (\nu_3/3+1), \\ \sigma(\nu \rightarrow \nu-1) &= A_{01} g(\nu, \nu) (\nu_3/3),\end{aligned}\quad (1)$$

where  $A_{01}$  is the cross section, integrated over the spectrum, for the absorption of the excited  $\nu_3$  mode on the fundamental transition ( $A_{01} = 2 \times 10^{-16}$  cm),  $g(\nu, \nu)$  is the form factor that determines the line shape of the single photon transition in the quasicontinuum, and  $\nu_3$  is the average number of photons in the  $\nu_3$  mode for a molecule in the state  $\nu$ . The growth of the cross section  $\sim \nu_3/3 + 1$  is due to the fact that the square of the dipole moment for upward transition in the IR active mode increases in the harmonic approximation in proportion to  $\nu_3/3 + 1$ .

The average number of photons in the  $\nu_3$  mode depends not only on the accumulated energy, but also on the manner in which the absorbed energy  $\bar{\nu}$  is distributed among the vibrational degrees of freedom. We shall assume that the energy is uniformly distributed among  $s$  degrees of freedom, three of which pertain to the  $\nu_3$  mode, and then  $\nu_3 = (3/s)\bar{\nu}$ .

Assume that the shape of the lines  $g(\nu, \nu)$  is governed by broadening of the excited state on account of the transverse relaxation in the quasicontinuum and has a Lorentz contour:

$$g(\nu, \nu) = \frac{X_2 \nu}{\pi [(\nu - \nu_0 - X_1 \nu)^2 + (X_2 \nu)^2]}, \quad (2)$$

whose shift  $X_1 \nu$  and half-width  $X_2 \nu$  increase linearly with increasing  $\nu$ , with proportionality coefficient  $X_1$  and  $X_2$ . The assumption that the contour has a Lorentz shape for transitions in the quasicontinuum was used earlier by Fuss<sup>16</sup> to simulate the excitation of SF<sub>6</sub> molecules in a strong IR field, and led to good agreement with a number of experimental data.

It is thus assumed in the model considered that the cross section of the transitions is determined uniquely by the molecule energy  $\nu$ , by the number  $s$  of degrees of freedom among which it is uniformly distributed, by the frequency  $\nu$ , and by the two molecular constants  $x_1$  and  $x_2$ , which determine the displacement and the broadening of the contour  $g(\nu, \nu)$ .

Within the framework of the now universally assumed model of incoherent excitation of polyatomic molecules, the dynamics of the excitation within the quasicontinuum region is described by the transport equation

$$\begin{aligned}dn(\nu)/dt &= (I/h\nu) [-\sigma(\nu \rightarrow \nu+1)n(\nu) - \sigma(\nu \rightarrow \nu-1)n(\nu) \\ &+ \sigma(\nu-1 \rightarrow \nu)n(\nu-1) + \sigma(\nu+1 \rightarrow \nu)n(\nu+1)],\end{aligned}\quad (3)$$

which goes over in the  $\nu \gg 1$  approximation into the diffusion equation

$$\begin{aligned}\frac{\partial n(\nu, \tau)}{\partial \tau} &= -\frac{\partial}{\partial \nu} \left[ \frac{n(\nu, \tau)}{\nu} \right] + \frac{\partial^2}{\partial \nu^2} \left[ \frac{1}{s-1} n(\nu, \tau) \right], \\ \nu &= \nu_{01}, \quad \tau = \frac{A_{01} X_2}{\pi (X_1^2 + X_2^2) h\nu} \int_{-\infty}^t I dt,\end{aligned}\quad (4)$$

where  $I$  and  $h\nu$  are the intensity and the quantum of the exciting field, and  $n(\nu, \tau)$  is the population of the quasicontinuum level in the vicinity of the energy  $\nu$ . We shall consider the situation of complete depletion of the lower levels. Then

$$\int_0^{\infty} n(\nu, \tau) d\nu = 1,$$

and with the aid of (4) we obtain the necessary boundary conditions:

$$\frac{n}{\nu} \Big|_{\nu=0} = \frac{1}{s-1} \frac{\partial n}{\partial \nu} \Big|_{\nu=0}.\quad (5)$$

At constant  $s$  we easily obtain for Eq. (4) a solution that tends to  $\delta(\nu - 0)$  at  $\tau \rightarrow 0$ . It is of the form

$$\begin{aligned}n(\nu, \tau) &= \left[ 2 \left( \frac{s-1}{4} \right)^{s/2+1} / \Gamma \left( \frac{s}{2} + 1 \right) \right] \\ &\times \left( \frac{\nu}{\tau^{1/2}} \right)^{s-1} \exp \left[ -\frac{(s-1)\nu^2}{4\tau} \right] \tau^{-1/2}.\end{aligned}\quad (6)$$

The distribution obtained differs from the thermal distribution

$$n_T(\nu, \Theta) = \frac{\nu^{s-1}}{\Theta^s (s-1)!} \exp \left( -\frac{s\nu}{\Theta} \right), \quad (7)$$

where  $\Theta = kT/h\nu$  and  $T$  is the temperature. At the same time, these differences are small. Thus, the ratio of the width  $\Delta\nu_{1/2}$  at half maximum to the position  $\nu_{\max}$  of the maximum of this distribution is determined for the distributions (7) and (6) by the expressions

$$\Delta\nu_{1/2}/\nu_{\max} = 2(\ln 2)^{1/2} (2/(s-1))^{1/2} \quad (8a)$$

for the thermal distribution (7) and

$$\Delta\nu_{1/2}/\nu_{\max} = 2(\ln 2)^{1/2} (1/(s-1)) \quad (8b)$$

for the distribution (6). We see from this that the distribution (6) at a fixed value  $s \gg 1$  is only 1.4 times narrower than thermal.

Using the distribution (6) obtained, we determine the average number  $\bar{\nu}$  of the photons absorbed by the molecules at the frequency of the exciting field  $\nu = \nu_{01}$ :

$$\bar{\nu} = \int \nu n(\nu, \tau) d\nu = \frac{\Gamma((s+1)/2)}{\Gamma(s/2)} \left[ \frac{4A_{01} X_2 \Phi}{\pi (s-1) (X_1^2 + X_2^2) h\nu} \right]^{1/2}, \quad (9)$$

or, for  $S \gg 1$ :

$$\bar{\nu} = [0.7A X_2 \Phi / h\nu (X_1^2 + X_2^2)]^{1/2}, \quad \Phi = \int I dt, \quad (10)$$

where  $\Phi$  is the energy density of the exciting pulse.

The character of the dependence  $\bar{\nu}(\Phi) \sim \Phi^{0.5}$  in expression (10) agrees well with the experimentally observed one (see Fig. 2) in the region  $\bar{\nu} \gg 1$ , and from the measured value  $\bar{\nu} = 15$  photon/molec. at  $\Phi_1 = 1$  J/cm<sup>2</sup> we obtain with the aid of (10)

$$|X_2| / (X_1^2 + X_2^2) \approx 1/26. \quad (11)$$

From the value  $|\nu_{\max} - \nu_0|/\bar{\nu} = 3.1$  cm<sup>-1</sup> measured at  $\bar{\nu} = 15$  (Fig. 9a) we obtain the estimate  $X_1 \approx -3.1$  cm<sup>-1</sup>, and from (11) we obtain  $X_2 \approx 0.4$  cm<sup>-1</sup>.

The obtained value of  $X_2$  is too small to account for the observed broadening of the linear absorption spectrum of the excited molecules. Consequently, the spectrum is made up of a superposition of many homogeneously broadened absorption lines, i.e., it is inhomogeneously broadened and reflects by the same token the distribution of the molecules over the energy levels.

The model considered above and the estimate of the constants  $X_1$  and  $X_2$  are not accurate enough for an unambiguous quantitative interpretation of the linear-absorption spectra and for the determination of the number of degrees of freedom and of the form of the molecule distribution over the levels under laser excitation. At the same time, the model does permit a quantitative treatment of the differences between the spectra obtained by heating and by laser excitation.

Indeed, in accordance with expression (8) the increase in the number of degrees of freedom over which energy is distributed leads to a decrease in the relative width of the distribution of the molecules over the energy levels and accordingly it should lead to a decrease in the width of the linear-absorption spectrum normalized to the number of absorbed photons.

In thermal heating of the gas, the number of degrees of freedom  $S_T$  increases with increasing temperature, since the number of vibrational modes for which the relation  $kT \gg h\nu_i$  is satisfied increases, and the temperature dependence of  $S_T$  takes the form

$$S_T = \frac{E(T)}{kT}, \quad E(T) = \sum_{i=1}^{15} \frac{h\nu_i}{\exp(h\nu_i/kT) + 1}. \quad (12)$$

The increase of  $S_T$  manifests itself in the fact that when the temperature is raised the normalized width  $\Delta\nu_{1/2}/\bar{\nu}$  of the thermal spectra decreases (see Fig. 9b, curve 2').

In laser excitation,  $\Delta\nu_{1/2}/\bar{\nu}$  also decreases with increasing number of absorbed photons and comes close to the half-width of the thermal spectra. The large half-width of the laser spectra cannot be explained within the framework of the model considered here as being due to the distribution of the molecules over the energy levels, since the model predicts a narrower distribution in this case. The observed differences can therefore be the consequence of only nonthermal distribution of the absorbed energy over the degrees of freedom of the molecules under laser excitation.

The number  $S_L$  of the degrees of freedom activated by laser excitation can be roughly estimated from the ratio of the half-width of the thermal and laser spectra. Estimates made under the assumption that by the instant of the sounding, owing to the collisions, the distribution of the molecules over the levels is close to thermal, yield values  $S_L = 5$  ( $\bar{\nu} = 5$ ),  $S_L = 6.5$  ( $\bar{\nu} = 10$ ) and  $S_L = 8$  ( $\bar{\nu} = 15$ ), noticeably smaller than the corresponding equilibrium values  $S_T = 8.5, 10.5,$  and  $11.5$  obtained from (12).

Thus, the foregoing analysis indicates that under laser excitation the distribution of the absorbed energy over the vibrational degrees of freedom of  $\text{SF}_6$  differs from the thermal equilibrium distribution, and these differences remain in force at least up to  $\nu = 15$  photon/molec.

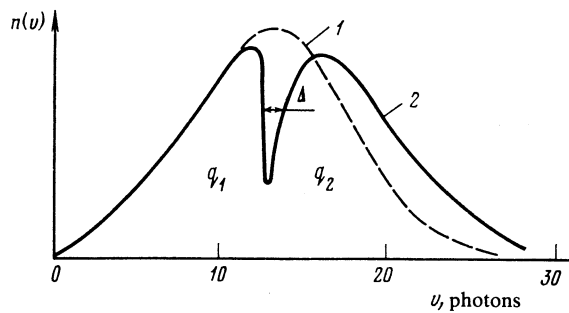


FIG. 10. Suggested form of the distribution of the molecules over the levels before (1) and after (2) the action of the second field.

The model discussed permits a qualitative explanation of the experimental results on two-frequency excitation of  $\text{SF}_6$ . Since the absorption contour of the molecules excited by the first field is inhomogeneous, the strong second field whose frequency  $\nu_2$  is shifted into the long-wave side of the frequency of the fundamental transition  $\nu_{01}$  enters into resonance with the molecules on the level  $v = |(\nu_2 - \nu_{01})/X_1|$ , excites them, and by the same time "burns a hole" in the distribution of the molecules over the levels. The qualitative picture of the change of the populations under the influence of the second field is shown in Fig. 10. The molecules break up into an ensemble of more highly excited molecules  $v > |(\nu_2 - \nu_{01})/X_1|$ , and an ensemble of less excited molecules,  $v < |(\nu_2 - \nu_{01})/X_1|$ . The fractions of the molecules in each of them are respectively  $q_2$  and  $q_1$ , with  $q_2 + q_1 = 1$ .

The dynamics of the excitation of the two ensembles reduces to two significant factors.

1) The initial fraction of the molecules in the second ensemble  $q_2$  is less than unity and is smaller the lower the excitation level in the first field and the larger the long-wave shift of the frequency of the second field. Since the width  $\sim X_2\nu$  of the contours of the single-photon transitions is larger for the molecules of the second ensemble, the second field being at resonance with a larger number of transitions excites primarily and dissociates the molecules of the second ensemble. The smaller the initial fraction  $q_2$  of the molecules and the larger the "red" shift of the frequency  $|\nu_2 - \nu_{01}|$ , the higher the dissociation quantum efficiency  $\beta$  calculated for all the  $\text{SF}_6$  molecules. This conclusion agrees well with the experimentally observed behavior of the  $W(\bar{\nu}_1 + \bar{\nu}_2)$  and  $\beta(\bar{\nu}_1 + \bar{\nu}_2)$  curves (see Figs. 6 and 7) with changing frequency  $\nu_2$  of the second field and with changing excitation level  $\bar{\nu}_1$  in the first field.

2) The molecules of the second ensemble, which absorb the energy of the second field mainly in the wings of the narrower contours, go over to the second ensemble. The molecule fraction  $q_1$  decreases, and when the energy density of the second field increases we have  $q_1 \rightarrow 0$ . All the molecules go over into the second ensemble and dissociate. This explains why at high excitation densities the observed  $W(\Phi_1, \Phi_2)$  dependence (see Fig. 5) saturates and the quantum efficiency of the dissociation becomes independent of the excitation method.

In addition, an appreciable contribution to the excitation of the molecules of the first ensemble can be made by the

fast  $V-V$  exchange of the molecules of the first ensemble with the more highly excited molecules, while the rate of the  $V-V$  relaxation can increase considerably with increasing vibrational excitation.

The foregoing subdivision into two ensembles of molecules in a quasicontinuum differs qualitatively from that carried out in Refs. 8 and 9 into "hot" and "cold" ensembles, a subdivision due to the differences between the spectra and the excitation dynamics of the system of lower levels and of the quasicontinuum levels.

The model considered is purely radiative in character and does not take into account the possible influence, under the experimental conditions, of longitudinal relaxation processes, such as rotational relaxation and rapid  $V-V$  exchange in the region of high vibrational states. An obvious development of the model is a clarification of the role played by the relaxation processes in the quasicontinuum, and allowance for these processes as well as, principally, for the  $V-V$  exchange between the excited molecules.

In addition, direct experiments must be performed to verify the limits of applicability of the model. Thus, for example, sounding of the dip predicted by the model in the populations of the levels in the case of two-frequency excitation (Fig. 10), using a third laser, will lead to a final conclusion concerning the relation between the homogeneous and inhomogeneous broadening in the quasicontinuum, and to a more accurate shape of the homogeneous line of the single-photon transition in the quasicontinuum.

## V. CONCLUSION

In conclusion, we formulate briefly the main results and deductions obtained in the paper.

1) We investigated the energy absorption and the dissociation probability of  $SF_6$  molecules in the single-frequency and two-frequency excitation regimes. A quantitative comparison of the results of these measurements was made.

2) The spectral dependences of the energy absorption and of the dissociation of  $SF_6$  in the two-frequency regime were obtained in the range of the second-field frequencies  $790-950\text{ cm}^{-1}$ .

3) The quantum efficiency of two-frequency dissociation of  $SF_6$  was seen to depend on the frequency of the second field and on the excitation level in the first field.

4) The maximum value of the quantum efficiency of dissociation of  $SF_6$ ,  $\beta = 0.7$ , was measured, and the level of overexcitation of the  $SF_6$  molecules, necessary to reach 100% dissociation, was determined.

5) The spectra of the linear absorption of an ensemble of  $SF_6$  molecules excited in a laser field to different levels were obtained.

6) A substantial difference was found between the parameters of these spectra and the thermal ones.

7) It was established that is no "cold" ensemble of  $SF_6$  molecules under the experimental conditions ( $T = 300\text{ K}$ ,

$P_{\Sigma} = 1\text{ Torr}$ ,  $\tau_3 = 1\text{ }\mu\text{sec}$ , and  $\Phi > 0.4\text{ J/cm}^2$ ).

8) A simple model of the dynamics of radiative excitation of molecules in a quasicontinuum was considered and the limits of its applicability discussed.

9) On the basis of the model developed, a treatment was presented of the experimentally observed deviations of the spectral parameters from thermal. It is shown that the homogeneous width of the contours of the single-photon transitions in the quasicontinuum is considerably narrower than the inhomogeneous width governed by the distribution of the  $SF_6$  molecules over the energy levels.

10) Analysis of the parameters of the spectra of the linear absorption of the excited molecules shows that under laser excitation of the gas the distribution of the absorbed energy over the vibrational degrees of freedom differs from the thermally equilibrium distribution.

11) Using the model developed it was shown that under conditions of two-frequency action the second field subdivides the molecules into two ensembles, whose excitation dynamics explains the experimentally observed dependence of the quantum efficiency of  $SF_6$  dissociation on the frequency of the second field and on the preliminary-excitation level.

The authors thank A. M. Prokhorov and N. V. Karlov for interest and support and also V. M. Akulin, S. M. Nikiforov, Sh. Sh. Nabiev, A. L. Shtarkov, and E. K. Karlova for a number of helpful discussions and for help with the experiments.

- <sup>1</sup>J. L. Steinfeld, I. Burak, and A. V. Nowak, *J. Chem. Phys.* **52**, 5421 (1970).  
<sup>2</sup>R. V. Ambartsumyan, Yu. A. Gorokhov, V. S. Letokhov, G. N. Makarov, A. A. Pureskii, and N. P. Furzikov, *Pis'ma Zh. Eksp. Teor. Fiz.* **23**, 217 (1976) [*JETP Lett.* **23**, 194 (1976)].  
<sup>3</sup>V. M. Akulin, S. S. Alimpiev, N. V. Karlov, A. M. Prokhorov, V. G. Sartakov, and E. M. Khokhlov, *ibid.* **25**, 428 (1977) [**25**, 400 (1977)].  
<sup>4</sup>B. I. Vasil'ev, A. Z. Grasyuk, A. P. Dyad'kin, A. N. Sukhanov, and A. B. Yastrebkov, *Kvant. Elektron. (Moscow)* **7**, 116 (1980) [*Sov. J. Quantum Electron.* **10**, 64 (1980)].  
<sup>5</sup>S. S. Alimpiev, *Izv. AN SSSR, Ser. Fiz.* **45**, 1070 (1981).  
<sup>6</sup>G. Koren, M. Dahan, and U. P. Oppenheim, *IEEE J. Quant. Electr.* **QE16**, 1380 (1980).  
<sup>7</sup>Yu. R. Kolomiiskii, A. R. Kukhudzhanov, and E. A. Ryabov, *Kvant. Elektron. (Moscow)* **7**, 1499 (1980) [*Sov. J. Quantum Electron.* **10**, 863 (1980)].  
<sup>8</sup>R. V. Ambartsumian, G. N. Makarov, and A. A. Puresky, *Opt. Commun.* **27**, 79 (1978).  
<sup>9</sup>V. N. Bagratishvili, V. S. Dolzhikov, and V. S. Letokhov, *Zh. Eksp. Teor. Fiz.* **76**, 18 (1979) [*Sov. Phys. JETP* **49**, 8 (1979)].  
<sup>10</sup>I. O. Leipunskii, A. K. Lyubimova, A. A. Nadeikin, A. I. Nikitin, and V. L. Tal'roze, *Kvant. Elektron. (Moscow)* **9**, 668 (1982) [*Sov. J. Quantum Electron.* **12**, 413 (1982)].  
<sup>11</sup>J. L. Lyman, *J. Chem. Phys.* **67**, 1868 (1977).  
<sup>12</sup>A. S. Sudbo, P. A. Schulz, E. R. Grant, Y. R. Shen, and Y. T. Lee, *J. Chem. Phys.* **69**, 2312 (1978); **72**, 4958 (1980).  
<sup>13</sup>P. N. Schatz and P. F. Hornig, *J. Chem. Phys.* **21**, 1516 (1953).  
<sup>14</sup>A. V. Nowak and J. L. Lyman, *J. Quant. Spectr. Rad. Transf.* **15**, 945 (1975).  
<sup>15</sup>J. F. Bott, *Appl. Phys. Lett.* **32**, 624 (1978).  
<sup>16</sup>W. Fuss, *Chem. Phys.* **36**, 135 (1979).

Translated by J. G. Adashko